Inorganic Chemistry

Article

pubs.acs.org/IC

A Study on the Effect of Dianionic Tridentate Ligands on the Radiative and Nonradiative Processes for Gold(III) Alkynyl Systems by a Computational Approach

Elizabeth Suk-Hang Lam, Wai Han Lam,* and Vivian Wing-Wah Yam*

Department of Chemistry, The University of Hong Kong, Pokfulam Road, Hong Kong, P. R. China

Supporting Information

ABSTRACT: Gold(III) alkynyl complexes with dianionic tridentate pincer ligands have received growing attention recently because of their rich luminescence behavior and their potential applications in areas such as optoelectronics and sensors. In this study, density functional theory (DFT) and time-dependent DFT (TDDFT) calculations have been performed to investigate the radiative and nonradiative processes for the gold(III) alkynyl complexes with different dianionic tridentate ligands, [Au(C^N^C)(C≡CC$_6$H$_5$)] (**1**; C^N^C = 2,6-diphenylpyridine), [Au(C(Np)^N^C(Np))(C≡CC$_6$H$_5$)] [**2**; C(Np)^N^C(Np) = 2,6-di(2-naphthyl)pyridine], [Au(N^N^N)(C≡CC$_6$H$_5$)] [**3**; N^N^N = 2,6-bis(benzimidazol-2′-yl)pyridine], and [Au(C^C^N)(C≡CC$_6$H$_5$)] [**4**; C^C^N = 3-(2-pyridyl)biphenyl]. It has been found that the electronic properties of the tridentate ligand could have a significant impact on the radiative and nonradiative processes. This study provides an in-depth understanding on the effect of the dianionic pincer ligands on the different photophysical behaviors among the gold(III) alkynyl complexes and crucial information for the future design of gold(III) complexes in various applications.

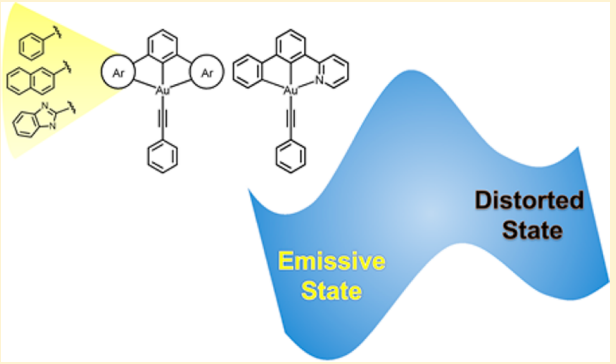

INTRODUCTION

Gold(III) chemistry has aroused interest over the past few decades because these complexes have been utilized in materials science,[1] medicine,[2] and catalysis.[3] However, because of the rather electrophilic nature of gold(III) center, which could be readily reduced, gold(III) complexes, in the absence of electron-rich ligands, are considered to be relatively unstable and susceptible to reductive elimination, which has limited the development of gold(III) chemistry.[4] In order to have structurally and chemically robust gold(III) complexes, the use of electron-rich tridentate ligands has been extensively explored because of its rigid ligand framework.[5] It is also believed that the incorporation of strong σ-donating coordinating ligands would render the gold(III) center more electron-rich, hence disfavoring reductive elimination.[6] Gold(III) complexes with tridentate ligands have been demonstrated to exhibit rich photophysical properties, leading to applications in diverse areas such as organic light-emitting diodes (OLEDs),[1a,b,7] organic solar cells,[8] and sensors.[9]

The choice of the tridentate ligand has a strong influence on the photophysical properties of the gold(III) complexes. The gold(III) complexes with neutral terpyridine ligand in aqueous solution were reported in 1983.[10] Subsequently, gold(III) complexes with N-heterocyclic carbene ligands, 2,6-bis(imidazol-2-yl)pyridine and 2,6-bis(benzimidazol-2-yl)pyridine, have been developed and found to be nonemissive in both the solid state and solution.[11] With the introduction of a stronger σ-donating anionic tridentate ligand, gold(III) complexes with 6-phenyl-2,2′-bipyridine ligands has been developed.[12] Upon incorporation with alkynyl ligands, these gold(III) 6-phenyl-2,2′-bipyridine complexes were found to be emissive in glass and the solid state, yet they are still nonemissive in solution.[12]

Dianionic tridentate ligands have been explored in gold(III) coordination chemistry because the dianionic ligand can stabilize the electrophilic gold(III) center.[13] In particular, cyclometalated dianionic ligands are popular pincer ligands because of the presence of strong carbon donors, which can render the gold(III) center more electron-rich,[7a,b,14] as well as the relatively high Au−C bond energy, leading to stable gold aryl complexes.[15] The class of gold(III) complexes with the 2,6-diphenylpyridine (C^N^C) ligand is one of the promising systems with two anionic carbon donors.[5a,13a] The gold(III) alkynyl complexes with simple 2,6-diphenylpyridine ligands, [Au(C^N^C)(C≡CR)], have been observed to emit green light in solution at room temperature.[14a] It has been demonstrated that the photophysical properties of these gold(III) complexes can be varied with modification of the C^N^C ligand or by the incorporation of different alkynyl ligands.[1a,7b,c] For example, tunable emission can be achieved by the introduction of an extended π-conjugated C^N^C ligand.[7b] It is also noted that [Au(C(Np)^N^C(Np))(C≡CC$_6$H$_4$OMe-

Received: January 28, 2015
Published: March 18, 2015

DOI: 10.1021/acs.inorgchem.5b00215
Inorg. Chem. 2015, 54, 3624−3630

p)] [C(Np)^N^C(Np) = 2,6-di(2-naphthyl)pyridine] has a higher photoluminescence quantum yield in solution than its C^N^C counterpart.[7b] With these rich and interesting photophysical properties, [Au(C^N^C)(C≡CR)] complexes and their derivatives have been employed in efficient OLED applications.[1a,b,7a−c,e]

While cyclometalated gold(III) complexes with dianionc C^N^C ligands have received much attention and have been extensively studied,[1b,7a−c,14a,b] gold(III) complexes with dianionic pure nitrogen-donor ligands of 2,6-bis(1*H*-benzimidazol-2-yl)pyridine have only received limited attention.[2b,8a,10] This class of complexes can display interesting sol−gel properties that can be utilized in biological sensing applications upon coordination to appropriate alkynyl ligands.[8a] Yet, in contrast to the cyclometalated gold(III) alkynyl complexes, gold(III) alkynyl complexes with 2,6-bis(benzimidazol-2′-yl)-pyridine ligands are nonemissive in solution, the solid state, and glass. It is believed that the lack of rich luminescence behavior could be accounted for by the presence of the low-energy deactivating excited states involving population to the metal−ligand antibonding orbital (dσ*),[6] which would result in significant molecular distortion, facilitating the nonradiative decay processes.

It has been observed that the tridentate dianionic ligands play a crucial role in determining the photophysical behavior of the gold(III) complexes. Information on both radiative and nonradiative processes are essential for a better design of the complexes for optical and sensing applications. Although several computational studies have been performed for octahedral transition-metal complexes to investigate the reaction energy profile for the conversion from triplet metal-to-ligand charge transfer (^{3}MLCT) excited state to triplet metal-centered (^{3}MC) excited state, which is considered to be one of the effective nonradiative pathways,[16] there were no reports on the investigation in square-planar complexes until very recently when Yam and co-workers have revealed for the first time the potential energy profiles for the thermal deactivation process via the ^{3}MC state of square planar platinum(II) alkynyl complexes with tridentate ligand.[17] Meanwhile, computational studies on the radiative and nonradiative process of gold(III) complexes have been scarce.[18] Because of the promising applications of the gold(III) complexes,[1,2b,7a−d,8,9,12] it is important to investigate how the nature of the tridentate ligands would affect the excited-state processes. In addition, although it is believed that the introduction of a strong carbon donor to the gold center could raise the energy of the nonemissive distorted state,[6] the effect of the position of the carbon donors in the pincer ligand on the radiative and nonradiative processes is unclear.

Herein, computational studies are performed to study four representative gold(III) arylalkynyl complexes with dianionic pincer ligands. The gold(III) phenylalkynyl complex of the 2,6-diphenylpyridine ligand, [Au(C^N^C)(C≡CC$_6$H$_5$)] (**1**) and its analogue with the more π-conjugated C^N^C ligand 2,6-di(2-naphthyl)pyridine, [Au(C(Np)^N^C(Np))(C≡CC$_6$H$_5$)] (**2**), are selected to elucidate the effect of extended π conjugation of the ligand on their photophysical behaviors. To study how the electron-donating ability of the tridentate ligands would influence the excited-state properties, the complex with the dianionic nitrogen-donor ligand 2,6-bis(1*H*-benzimidazol-2-yl)pyridine, [Au(N^N^N)(C≡CC$_6$H$_5$)] (**3**), has also been investigated. In addition, a hypothetical gold(III) complex with the 3-(2-pyridyl)biphenyl (C^C^N) ligand, [Au(C^C^N)(C≡CC$_6$H$_5$)] (**4**), which has not been reported experimentally, has also been included (Scheme 1) to study the effect of the positions of the carbon rings in the pincer ligand on the excited-state processes. This study would provide important insight into the different photophysical behaviors among the gold(III) complexes with dianionic tridentate ligands and provide crucial information for the future design of gold(III) complexes for sensing and photonic applications.

Scheme 1. Chemical Structures of the Complexes Presented in This Study

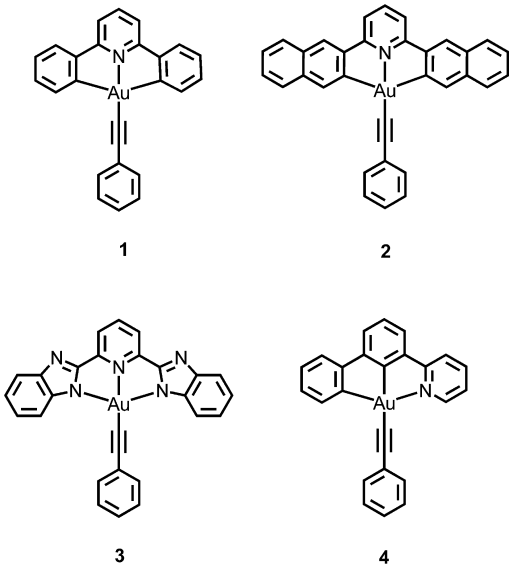

COMPUTATIONAL DETAILS

All of the density functional theory (DFT) and time-dependent DFT (TDDFT) calculations were carried out with *Gaussian09* software.[19] Geometry optimizations were performed for the ground states, triplet excited states, and transition states (TSs) using DFT with the hybrid Perdew, Burke, and Ernzerhof functional[20] in conjunction with the conductor-like polarizable continuum model (CPCM) in CH_2Cl_2.[21] The unrestricted formalism was used for the triplet states. TDDFT calculations with the Tamm−Dancoff approximation have been performed at the ground-state and lowest-energy triplet excited-state geometries in order to have a better estimation of the excitation energies.[22] Vibrational frequencies were calculated for all stationary points to verify that each was a minimum (NIMAG = 0) or a TS (NIMAG = 1) on the potential energy surface. Intrinsic reaction coordinate calculations were also carried out to confirm the TSs connecting two relevant minima.[23] The minimum-energy crossing points between the relevant potential energy surfaces were optimized using *Gaussian09*, together with the code developed by Harvey et al.[24] For all calculations, the Stuttgart effective core potentials and associated basis set were applied to describe gold[25] with f-type polarization functions (ζ = 1.050),[26] whereas for all other atoms, the 6-31G(d,p) basis set[27] was used.

RESULTS AND DISCUSSION

Gold(III) alkynyl complexes with C^N^C and N^N^N ligands have been shown to exhibit different photophysical properties.[7a,b,8a,14a] The [Au(N^N^N)(C≡CR)] complexes are generally nonemissive in solution, glass, and the solid state, while the gold(III) complexes of the nonsubstituted 2,6-diphenylpyridine ligand, [Au(C^N^C)(C≡CR)], exhibit a vibronic-structured emission in solution.[8a,14a] On the other hand, [Au(C(Np)^N^C(Np))(C≡CC$_6$H$_4$OMe-*p*)] has been

DOI: 10.1021/acs.inorgchem.5b00215
Inorg. Chem. 2015, 54, 3624−3630

reported to emit yellow with a higher photoluminescence quantum yield than [Au(C^N^C)(C≡CC$_6$H$_4$OMe-*p*)] involving the simple C^N^C ligand.[14a] To gain a better understanding of the different emissive behaviors, **1**−**3** are chosen for the present study.

TDDFT calculations have been performed for complexes **1**−**3** at their respective ground-state-optimized geometries, in order to gain a better insight into the nature of the triplet excited states. Table 1 lists selected singlet−triplet transitions for all complexes, and the molecular orbitals involved in the transitions of **1**−**3** are shown in Figures 1 and 2 and S1 in the Supporting Information (SI). Because the emission of a given spin multiplicity usually originates from the lowest-energy excited-state level of that spin multiplicity, as stated in Kasha's rule,[28] the T_1 state is assumed to be the emissive state (^{3}ES) for the discussions below. The T_1 state of complexes **1**−**3** is predominantly the intraligand ^{3}IL[$\pi\rightarrow\pi^*$] state of the tridentate ligand with some charge-transfer character from the two peripheral rings to the central pyridine unit (Table 1). Because of the extended π conjugation of the C^N^C ligand in **2** compared to **1**, the transition is found to be red-shifted in energy by 1774 cm^{-1} in **2**, which is in line with the trend observed from the experimental finding.[7b,14a]

Table 1. Selected Singlet−Triplet Transitions for 1−4 at Their Ground-State-Optimized Geometries Computed by TDDFT/CPCM Calculations

complex	T_n	excitation[a]	coefficient[b]	vertical excitation energy/eV
1	T_1[c]	H−1 → L	0.67	2.89
	T_{13}[d]	H−2 → L+3	0.66	4.30
2	T_1[c]	H → L+1	0.53	2.67
	T_{19}[d]	H−4 → L+5	0.54	4.32
3	T_1[c]	H → L	0.63	2.69
	T_4[d]	H−1 → L+1	0.52	2.89
4	T_1[c]	H−1 → L+1	0.38	2.99
	T_9[d]	H → L+3	0.52	4.22

[a]The orbitals involved in the excitations (H = HOMO and L = LUMO). [b]The largest coefficient in the configuration interaction expansion. [c]The excited state is the predominant ^{3}IL state of the tridentate ligand. [d]The distorted state.

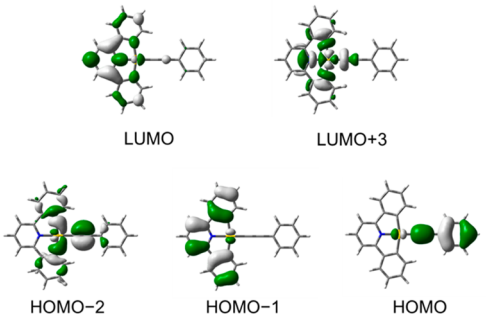

Figure 1. Spatial plots (isovalue = 0.03) for selected molecular orbitals of **1**.

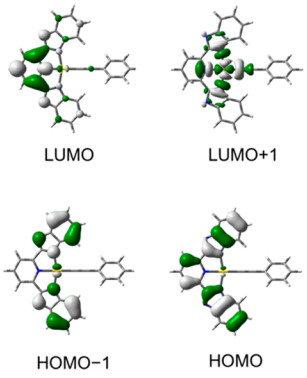

Figure 2. Spatial plots (isovalue = 0.03) for selected molecular orbitals of **3**.

Radiative Process. Geometry optimizations of the lowest-energy triplet excited state for **1**−**3** have been performed. The spin density of complexes **1**−**3** is mainly localized on the tridentate ligand, as depicted in Figure 3. The radiative decay

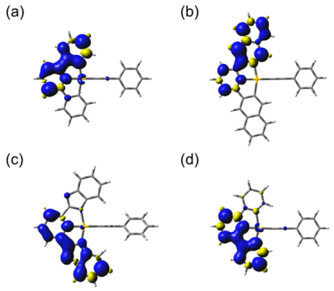

Figure 3. Plots of the spin density (isovalue = 0.002) of the ^{3}ESs for (a) **1**, (b) **2**, (c) **3**, and (d) **4**.

rate constant (k_r) is calculated according to the method reported previously.[17] There are three factors governing the radiative rate constant under the formalism, namely, the strength of the spin−orbit coupling interaction $\langle S_n|H_{SOC}|T_1\rangle$ between the higher-lying singlet excited states (S_n) and ^{3}ES, the oscillator strength (f) of the S_n states that can couple with ^{3}ES, and the energy separation between the coupled states.[17] As the spin−orbit coupling interaction is approximated by the sum of one-particle operators,[30] the metal contribution involved in the excited states is the dominant factor in determining the spin−

DOI: 10.1021/acs.inorgchem.5b00215
Inorg. Chem. 2015, 54, 3624−3630

orbit interaction. Because the spin−orbit coupling constant (ξ = 5093 cm^{-1})[31] for gold is larger than that for other atoms, spin−orbit coupling involving atoms other than gold is neglected. Selected singlet−singlet and singlet−triplet transitions at the T_1-optimized state are listed in Tables S1−S5 in the SI.

The calculated radiative rate constant follows a trend of **1** > **2** > **3**, as shown in Table 2. The radiative decay rate constants for

Table 2. Calculated Radiative Decay Rate Constants of the T_1 State for 1−4

complex	k_r/s^{-1}
1	6.73×10^3
2	6.06×10^2
3	5.29×10^2
4	8.41×10^2

1 and an analogue complex of **2**, [Au(C(Np)^N^C(Np))(C≡CC$_6$H$_4$OMe-*p*)], were estimated to be on the order of 10^{-4} and 10^{-3} s^{-1} on the basis of the measured photoluminescence quantum yield and lifetime. When the methoxy analogues of **1** and **2**, [Au(C^N^C)(C≡CC$_6$H$_4$OMe-*p*)] and [Au(C(Np)^N^C(Np))(C≡CC$_6$H$_4$OMe-*p*)], are compared, k_r in the former is one order of magnitude higher than that in the latter. Although the experimental k_r values cannot be reproduced with high precision, the difference in the order of magnitude between the corresponding methoxy analogues of **1** and **2** is in line with our calculated values.[7a,b] The metal contribution in the ^{3}ES, as indicated by the *c* coefficient of d orbitals involved in the excitation in the ^{3}ES, also has the same trend of **1** > **2** > **3** (Figures S2a−c in the SI). Therefore, a smaller metal participation in **2** and **3** in the ^{3}ES is attributed to a smaller calculated k_r relative to **1**. Because the tridentate ligands of **2** and **3** are more π-conjugated compared to that of **1**, a smaller metal contribution is found in the π orbital of the tridentate ligands, leading to a relatively small metal participation in the ^{3}ESs of **2** and **3**. Compared to the calculated k_r for platinum(II) complexes with tridentate pincer ligands investigated by Yam and co-workers recently,[17] a smaller k_r value was found for these gold(III) complexes because the metal d orbital participation is relatively smaller in their ^{3}ESs.

Nonradiative Process via the ^{3}DS. Because the electronic properties of the tridentate ligand are significantly affected by the nonradiative processes via the ^{3}DS for the gold(III) complexes, which play an important role in their excited-state properties, the study of the potential energy profiles of the deactivation processes is crucial to providing a deeper insight into the effect of the tridentate ligand on the deactivation process and directions for the better design of gold(III) materials.

Geometry optimizations of the lowest-energy ^{3}DSs for **1**−**3** have been performed and the spin density plots of the ^{3}DSs are depicted in Figure 4. All of the Au−C and Au−N bond distances of the tridentate ligands are lengthened in the ranges of 0.135−0.193, 0.133−0.212, and 0.162−0.320 Å for **1**−**3** relative to their respective ^{3}ESs. Selected optimized structures for the deactivation process are shown in Figures 5 and 6 and S3−S4 in the SI. For the C^N^C complexes **1** and **2**, in contrast to the ^{3}ES and S_0 state, which have planar structures, the ^{3}DSs of **1** and **2** are nonplanar, in which the two peripheral carbon rings of the tridentate ligand are bending down, while the central pyridine ring and alkynyl ligand are slightly bending

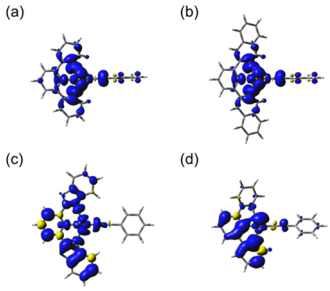

Figure 4. Plots of the spin density (isovalue =0.002) of the ^{3}DSs for (a) **1**, (b) **2**, (c) **3**, and (d) **4**.

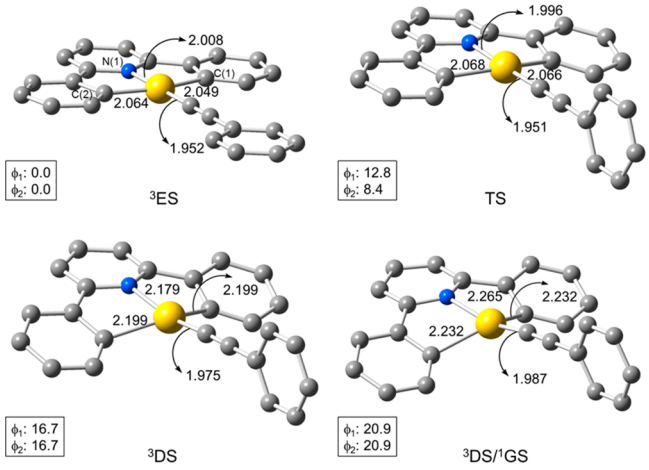

Figure 5. Optimized structures of ^{3}ES, TS, ^{3}DS, and ^{3}DS/^{1}GS for **1** with selected structural parameters, in which ϕ_1 and ϕ_2 are the interplanar angles between the C(1) and N(1) rings as well as the C(2) and N(1) rings, respectively (bond distances in anstroms and angles in degrees). Hydrogen atoms are omitted for clarity.

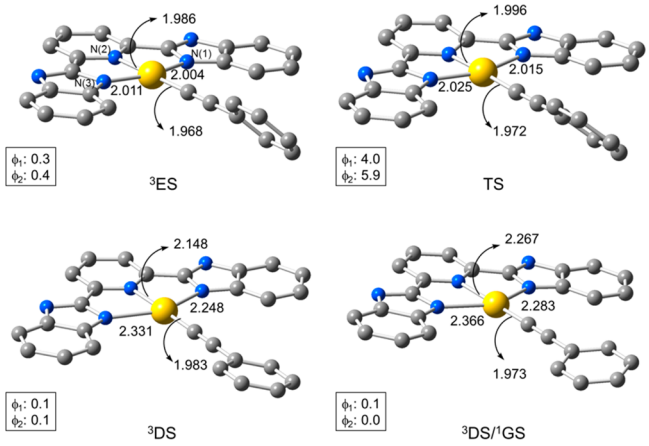

Figure 6. Optimized structures of ^{3}ES, TS, ^{3}DS, and ^{3}DS/^{1}GS for **3** with selected structural parameters, in which ϕ_1 and ϕ_2 are the interplanar angles between the N(1) and N(2) rings as well as the N(3) and N(2) rings, respectively (bond distances in anstroms and angles in degrees). Hydrogen atoms are omitted for clarity.

up (Figures 5 and S3 in the SI). The C(1)−Au−C(2) and N(1)−Au−C(alkynyl) bond angles are decreased by 25.0−26.0 and 12.4−13.3° relative to the ^{3}ES, respectively. Such tetrahedral distortion is compatible with 5d-6p orbital mixing.[32] As indicated by Mulliken population analysis, an increase in the metal p orbital contribution of **1** and **2** to the dσ* orbital in the

DOI: 10.1021/acs.inorgchem.5b00215
Inorg. Chem. 2015, 54, 3624−3630

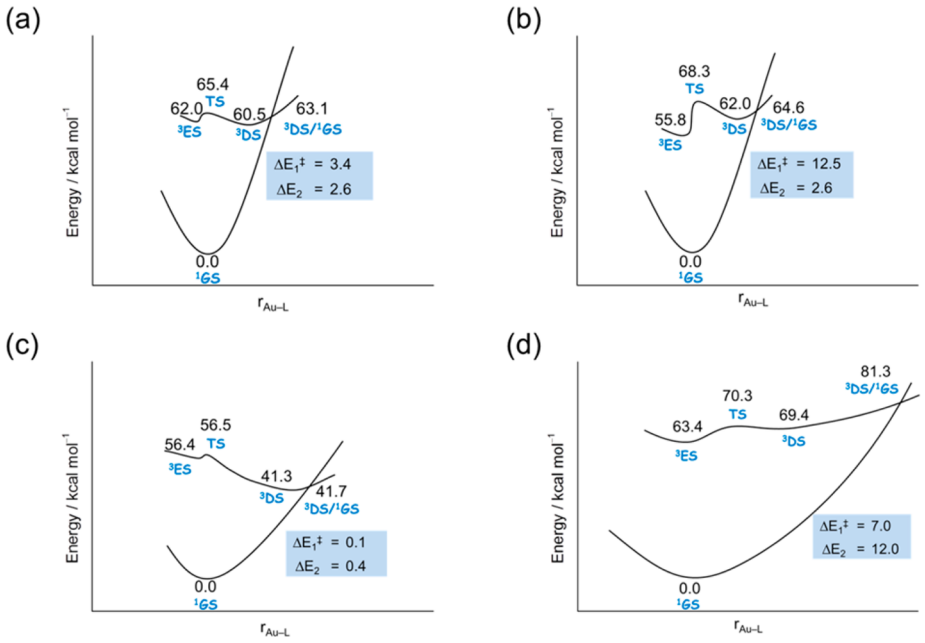

Figure 7. Schematic potential energy profiles of the deactivation pathway via the ^{3}DS for (a) **1**, (b) **2**, (c) **3**, and (d) **4**. $\Delta E_1^{\ddagger}$ is the activation energy from the ^{3}ES to the ^{3}DS, while ΔE_2 is the energy required to reach the ^{3}DS/^{1}GS.

^{3}DS is found relative to that in their corresponding S_0 state (Table S6 in the SI). In contrast to **1** and **2**, the ^{3}DS of **3** remains planar in structure, in which the metal p orbital contribution in the ^{3}DS of **3** is comparable to that in its S_0 state. The spin density of the ^{3}DSs of **1**−**3** is mainly localized on the metal center and tridentate ligand (Figures 4a−c). The Mulliken atomic spin density for the ^{3}DS at the gold(III) center for **1**−**3** is in the range of 0.43−0.51, which is much larger than that found in their corresponding ^{3}ESs (0.01−0.05).

The ^{3}DS of **1** lies lower in energy than the ^{3}ES by 1.5 kcal mol^{-1}. On the other hand, the ^{3}DS of **2** is 6.2 kcal mol^{-1} higher in energy than the ^{3}ES because of the presence of a lower-energy ^{3}ES as a result of the extended π conjugation of the C^N^C ligand. It is noted that the relative energy of the ^{3}DS in **3** with respect to the ground state (41.3 kcal mol^{-1}) is much smaller than those for **2** and **3** (60.5 and 62.5 kcal mol^{-1}) because of the presence of a lower-lying dσ* orbital in **3** and hence a lowering of the energy of the ^{3}DS. It is noted that the ^{3}DS in **3** is significantly lower in energy (15.1 kcal mol^{-1}) than the ^{3}ES.

The TS connecting the ^{3}ES and ^{3}DS of **1**−**3** has been found. The plots of the spin density for the TSs are depicted in Figures S5a−c in the SI. For all complexes, the Au−C and Au−N bond distances of the tridentate ligands are increased along the ^{3}ES → ^{3}DS conversion. In addition, the spin density for the gold center in the ^{3}DS is increased to 0.06−0.13 compared to its corresponding ^{3}ES. Complexes **1** and **2** have nonplanar TS structures, in which the average interplanar angles between the central ring and the two peripheral rings of the C^N^C ligand are 10.6 and 9.1°, respectively. On the other hand, the TS of **3** has almost a planar structure with the Au−N bond distances slightly lengthened by 0.004−0.021 Å, which resembles the structure of the ^{3}ES.

The feasibility of decaying back to the ground state after reaching the ^{3}DS is investigated by the minimum-energy crossing point (^{3}DS/^{1}GS) between the ^{3}DS and the ^{1}GS potential surfaces. The Au−C bond distances of the tridentate ligands in the crossing point are slightly lengthened for the C^N^C complexes **1** and **2** compared to that of the ^{3}DS. Contrary to **1** and **2**, in which their crossing points reveal a nonplanar structure, the ^{3}DS/^{1}GS crossing point of **3** possesses a planar structure. The spin density plots of the triplet state at the ^{3}DS/^{1}GS geometry for **1**−**3** are depicted in Figures S6a−c in the SI.

The potential energy profiles for the deactivation processes of **1**−**3** are shown in Figures 7a−c. The schematic plots are constructed with the electronic energy of the optimized ground and excited states [S_0, ^{3}ES, TS(^{3}ES−^{3}DS), and ^{3}DS] and ^{3}ES/^{1}GS point along the relative change of the metal−ligand bond distances (Au−L) of the tridentate units with respect to those in the ground state. As depicted in Figure 7a, the activation energy from the ^{3}ES to the ^{3}DS of **1** is 3.4 kcal mol^{-1}, and the ^{3}DS/^{1}GS point lies 2.6 kcal mol^{-1} above the ^{3}DS. The activation barrier for **2** is about 4 times higher (12.5 kcal mol^{-1}) than that for **1**. Although the ^{3}DS/^{1}GS crossing point for **2** lies above the ^{3}DS with an energy similar to that of **1**, the deactivation process in **2** is still less favorable with a higher activation barrier. With the nitrogen-donor ligand in **3**, the activation energy from the ^{3}ES to the ^{3}DS (0.1 kcal mol^{-1}) is very small, suggesting that the conversion is barrierless. In addition, the ^{3}DS/^{1}GS crossing point is located 0.4 kcal mol^{-1} above the ^{3}DS, indicating that **3** can easily return to the ^{1}GS once the ^{3}DS is populated. The nonemissive nature of **3** is possibly attributed to the negligible energy barrier along the deactivation pathway. It is anticipated that dianionic 2,6-bis(1*H*-benzimidazol-2-yl)pyridine is a poor electron-donating ligand, which makes the gold(III) center highly electrophilic and facilitates the deactivation process.

Position of the Carbon Rings. In order to study the effect of the position of the carbon ring in the tridentate ligand, the electronic structures of the ground and excited states of the hypothetical complex **4**, in which the phenyl ring is positioned in the central position while the pyridine ring is placed in the lateral position, have been studied. The T_1 state of **4** obtained

DOI: 10.1021/acs.inorgchem.5b00215
Inorg. Chem. 2015, 54, 3624−3630

from TDDFT calculations at the ground-state geometry is mainly the intraligand ^{3}IL[$\pi\rightarrow\pi^*$] state of the tridentate ligand. In contrast to **1**, in which the ^{3}DS is contributed by excitation from the σ-bonding orbital of the Au−C(phenyl) bonds to the dσ^* orbital, the ^{3}DS in **4** is mainly composed of excitation from the π orbital of the alkynyl and C^C^N ligands to the dσ^* orbital (Figure 8 and Table 1).

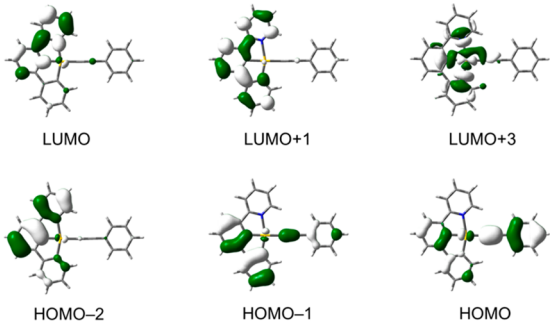

Figure 8. Spatial plots (isovalue = 0.03) for selected molecular orbitals of **4**.

It is noted that the energy of the optimized ^{3}ES of **4** relative to its ground state is slightly higher than that of **1**, indicating that the position of the phenyl rings in the tridentate ligand does not have a large impact on the energy of the ^{3}ES. The spin density at the ^{3}ES is mainly localized on the C^C^N ligand, as shown in Figure 3d. The radiative decay rate for **4** is listed in Table 2. Because **4** has only a few available singlet excited states that could effectively couple with ^{3}ES and a larger energy gap $\Delta E(S_n-{}^3ES)$, as well as a smaller metal contribution compared with **1**, it has a smaller calculated k_r.

The ^{3}DS of **4** has a nonplanar structure, in which a larger distortion from planarity between the lateral pyridine and central benzene rings is found than that between the central and lateral benzene rings (Figure S4 in the SI). Similar to **1** and **2**, an increase in the metal p orbital contribution to the dσ^* orbital in the ^{3}DS of **4** is found relative to that in the S_0 state (Table S6 in the SI). Compared to the ^{3}ES geometry, the Au−C and Au−N bonds in the ^{3}DS of **4** are lengthened by 0.07−0.15 and 0.71 Å, respectively. The spin density of the ^{3}DS is mainly localized on the metal and C^C^N ligand (Figure 4d). In contrast to **1**, where its ^{3}DS is lower in energy than the ^{3}ES, the ^{3}DS of **4** is higher in energy than the ^{3}ES by 6.0 kcal mol^{-1}.

The TS connecting ^{3}ES and ^{3}DS has been located for **4**, and the plot of the spin density is shown in Figure S5d in the SI. With regard to the structural changes, the Au−L bond distances of **4** are lengthened along the ^{3}ES → ^{3}DS conversion path by 0.04−0.30 Å. The activation barrier for the ^{3}ES → ^{3}DS conversion is 7.0 kcal mol^{-1}, which is 2 times larger than that of **1**. The ^{3}DS/^{1}GS of **4** shows a geometry change, with the pyridine and phenyl rings further twisted relative to the central phenyl ring by 14.2 and 12.0°, respectively (Figure S4 in the SI). The spin density of the triplet excited state at the ^{3}DS/^{1}GS is shown in Figure S6d in the SI.

The potential energy profile for complex **4** is presented in Figure 7d. Compared to **1**, **4** has a larger activation barrier from ^{3}ES to ^{3}DS, suggesting that the population to the ^{3}DS is less favorable than **1**. In addition, once the ^{3}DS of **4** is populated, a greater energy is required in **4** (12.0 kcal mol^{-1}) to reach the ^{3}DS/^{1}GS point than that in **1** (2.6 kcal mol^{-1}). It is interesting to note that a larger activation barrier as well as a higher-energy ^{3}DS/^{1}GS crossing point is found for the complex with unsymmetric tridentate ligand C^C^N, which suggests that the nonradiative decay process via the DS can be hampered by changing the lateral carbon ring to the central position of the tridentate ligand.

CONCLUSION

In short, the radiative and nonradiative processes via the DS for the gold(III) complexes with dianionic pincer ligands have been illustrated. It has been shown that the cyclometalated gold(III) complexes possess a larger radiative rate constant compared to the complex with pure nitrogen-donor pincer ligands. The stronger donating ability of the carbon atom compared to the nitrogen atom increases the electron-richness of the gold(III) center. It is shown that the metal participation in the ^{3}ES is the dominating factor to determine the radiative decay rate constants in the gold(III) systems. In addition, the gold(III) complex with the pure nitrogen-donor pincer ligand should readily undergo a deactivation pathway via the ^{3}DS state upon photoexcitation due to the negligible energy required to reach the ^{3}DS and ^{3}DS/^{1}GS. It has also been shown that the position of the carbon rings in the pincer ligand has a small effect on the energy of the ^{3}ES. However, the deactivation process becomes less favorable by shifting the lateral phenyl ring to the central position. The information allows a better design on the tuning of the excited-state properties of gold(III) alkynyl chromophores.

ASSOCIATED CONTENT

Supporting Information

Selected singlet and triplet excited states computed by TDDFT/CPCM calculations at the T_1-optimized geometries, percentage contribution of the gold atomic orbitals, selected molecular orbitals, energy level diagrams of selected excited states, optimized structures with selected structural parameters, plots of the spin density of the TS and the triplet state at the ^{3}DS/^{1}GS geometry, and Cartesian coordinates for selected optimized structures. This material is available free of charge via the Internet at http://pubs.acs.org.

AUTHOR INFORMATION

Corresponding Authors

*E-mail: chsue@hku.hk.
*E-mail: wwyam@hku.hk.

Notes

The authors declare no competing financial interest.

ACKNOWLEDGMENTS

We acknowledge support from The University of Hong Kong under the URC Strategic Research Theme on New Materials. This work has been supported by the Theme-Based Research Scheme (Project T23-713/11) and a General Research Fund Grant (HKU 17302414) from the Research Grants Council of the Hong Kong Special Administrative Region, China. E.S.-H.L. acknowledges the receipt of a Postgraduate Studentship from The University of Hong Kong. We are grateful to the Information Technology Services of The University of Hong Kong for providing computational resources.

REFERENCES

(1) (a) Au, V. K.-M.; Wong, K. M.-C.; Tsang, D. P.-K.; Chan, M.-Y.; Zhu, N.; Yam, V. W.-W. *J. Am. Chem. Soc.* **2010**, *132*, 14273.

DOI: 10.1021/acs.inorgchem.5b00215
Inorg. Chem. 2015, 54, 3624−3630

(b) Wong, K. M.-C.; Zhu, X.; Hung, L.-L.; Zhu, N.; Yam, V. W.-W.; Kwok, H.-S. *Chem. Commun.* **2005**, 2906. (c) Lai, S.-L.; Wang, L.; Yang, C.; Chan, M.-Y.; Guan, X.; Kwok, C.-C.; Che, C.-M.; Kung, K. K.-Y.; Lo, V. K.-Y.; Ko, H.-M.; Li, G.-L.; Chan, P.-Y.; Leung, K.-C.; Zhou, Z.; Wang, M.-Z.; Che, C.-M.; Wong, M.-K.; Zou, T.; Lum, C. T.; Chui, S. S.-Y.; Che, C.-M. *Adv. Funct. Mater.* **2014**, *24*, 4655.

(2) (a) Sivaram, H.; Tan, J.; Huynh, H. V. *Organometallics* **2012**, *31*, 5875. (b) Zou, T.; Lum, C. T.; Chui, S. S.-Y.; Che, C.-M. *Angew. Chem., Int. Ed.* **2013**, *52*, 2930.

(3) (a) Boronat, M. R.; Corma, A.; González-Arellano, C.; Iglesias, M.; Sánchez, F. L. *Organometallics* **2009**, *29*, 134. (b) Kung, K. K.-Y.; Lo, V. K.-Y.; Ko, H.-M.; Li, G.-L.; Chan, P.-Y.; Leung, K.-C.; Zhou, Z.; Wang, M.-Z.; Che, C.-M.; Wong, M.-K. *Adv. Synth. Catal.* **2013**, *355*, 2055.

(4) (a) Komiya, S.; Ozaki, S.; Shibue, A. *J. Chem. Soc., Chem. Commun.* **1986**, 1555. (b) Schuster, O.; Schmidbaur, H. *Organometallics* **2005**, *24*, 2289. (c) He, X.; Yam, V. W.-W. *Coord. Chem. Rev.* **2011**, *255*, 2111. (d) Smith, D. A.; Roşca, D.-A.; Bochmann, M. *Organometallics* **2012**, *31*, 5998.

(5) (a) Bronner, C.; Wenger, O. S. *Dalton Trans.* **2011**, *40*, 12409. (b) Wing-Wah Yam, V.; Chung-Chin Cheng, E. In *Photochemistry and Photophysics of Coordination Compounds II*; Balzani, V., Campagna, S., Eds.; Springer: Berlin, 2007; Vol. *281*, p 269.

(6) Yam, V. W.-W.; Cheng, E. C.-C. *Chem. Soc. Rev.* **2008**, *37*, 1806.

(7) (a) Wong, K. M.-C.; Hung, L.-L.; Lam, W. H.; Zhu, N.; Yam, V. W.-W. *J. Am. Chem. Soc.* **2007**, *129*, 4350. (b) Au, V. K.-M.; Tsang, D. P.-K.; Wong, K. M.-C.; Chan, M.-Y.; Zhu, N.; Yam, V. W.-W. *Inorg. Chem.* **2013**, *52*, 12713. (c) Tang, M.-C.; Tsang, D. P.-K.; Chan, M. M.-Y.; Wong, K. M.-C.; Yam, V. W.-W. *Angew. Chem., Int. Ed.* **2013**, *52*, 446. (d) To, W.-P.; Chan, K. T.; Tong, G. S. M.; Ma, C.; Kwok, W.-M.; Guan, X.; Low, K.-H.; Che, C.-M. *Angew. Chem., Int. Ed.* **2013**, *52*, 6648. (e) Tang, M.-C.; Tsang, D. P.-K.; Wong, Y.-C.; Chan, M.-Y.; Wong, K. M.-C.; Yam, V. W.-W. *J. Am. Chem. Soc.* **2014**, *136*, 17861.

(8) (a) Yim, K.-C.; Lam, E. S.-H.; Wong, K. M.-C.; Au, V. K.-M.; Ko, C.-C.; Lam, W. H.; Yam, V. W.-W. *Chem.—Eur. J.* **2014**, *20*, 9930. (b) Au, V. K.-M.; Zhu, N.; Yam, V. W.-W. *Inorg. Chem.* **2013**, *52*, 558.

(9) Liu, H.-Q.; Cheung, T.-C.; Peng, S.-M.; Che, C.-M. *J. Chem. Soc., Chem. Commun.* **1995**, 1787.

(10) Hollis, L. S.; Lippard, S. J. *J. Am. Chem. Soc.* **1983**, *105*, 4293.

(11) Lu, W.; Chan, K. T.; Wu, S.-X.; Chen, Y.; Che, C.-M. *Chem. Sci.* **2012**, *3*, 752.

(12) Au, V. K.-M.; Lam, W. H.; Wong, W.-T.; Yam, V. W.-W. *Inorg. Chem.* **2012**, *51*, 7537.

(13) (a) Wong, K.-H.; Cheung, K.-K.; Chan, M. C.-W.; Che, C.-M. *Organometallics* **1998**, *17*, 3505. (b) Yam, V. W. W.; Choi, S. W.; Lai, T. F.; Lee, W. K. *Dalton Trans.* **1993**, 1001. (c) Li, C. K.-L.; Sun, R. W.-Y.; Kui, S. C.-F.; Zhu, N.; Che, C.-M. *Chem.—Eur. J.* **2006**, *12*, 5253. (d) Che, C.-M.; Sun, R. W.-Y. *Chem. Commun.* **2011**, *47*, 9554.

(14) (a) Yam, V. W.-W.; Wong, K. M.-C.; Hung, L.-L.; Zhu, N. *Angew. Chem., Int. Ed.* **2005**, *44*, 3107. (b) Au, V. K.-M.; Wong, K. M.-C.; Zhu, N.; Yam, V. W.-W. *J. Am. Chem. Soc.* **2009**, *131*, 9076. (c) Stoccoro, S.; Alesso, G.; Cinellu, M. A.; Minghetti, G.; Zucca, A.; Manassero, M.; Manassero, C. *Dalton Trans.* **2009**, 3467.

(15) Chan, C.-W.; Wong, W.-T.; Che, C.-M. *Inorg. Chem.* **1994**, *33*, 1266.

(16) (a) Borg, O. A.; Godinho, S. S. M. C.; Lundqvist, M. J.; Lunell, S.; Persson, P. *J. Phys. Chem. A* **2008**, *112*, 4470. (b) Fredin, L. A.; Pápai, M.; Rozsályi, E.; Vankó, G.; Wärnmark, K.; Sundström, V.; Persson, P. *J. Phys. Chem. Lett.* **2014**, *5*, 2066. (c) Alary, F.; Boggio-Pasqua, M.; Heully, J.-L.; Marsden, C. J.; Vicendo, P. *Inorg. Chem.* **2008**, *47*, 5259. (d) Österman, T.; Abrahamsson, M.; Becker, H.-C.; Hammarström, L.; Persson, P. *J. Phys. Chem. A* **2012**, *116*, 1041. (e) Österman, T.; Persson, P. *Chem. Phys.* **2012**, *407*, 76. (f) Heully, J.-L.; Alary, F.; Boggio-Pasqua, M. *J. Chem. Phys.* **2009**, *131*, 184308.

(17) Lam, W. H.; Lam, E. S.-H.; Yam, V. W.-W. *J. Am. Chem. Soc.* **2013**, *135*, 15135.

(18) Yang, B.-Z.; Zhou, X.; Liu, T.; Bai, F.-Q.; Zhang, H.-X. *J. Phys. Chem. A* **2009**, *113*, 9396.

(19) Frisch, M. J.; Trucks, G. W.; Schlegel, H. B.; Scuseria, G. E.; Robb, M. A.; Cheeseman, J. R.; Scalmani, G.; Barone, V.; Mennucci, B.; Petersson, G. A.; Nakatsuji, H.; Caricato, M.; Li, X.; Hratchian, H. P.; Izmaylov, A. F.; Bloino, J.; Zheng, G.; Sonnenberg, J. L.; Hada, M.; Ehara, M.; Toyota, K.; Fukuda, R.; Hasegawa, J.; Ishida, M.; Nakajima, T.; Honda, Y.; Kitao, O.; Nakai, H.; Vreven, T.; Montgomery, J. A.; Peralta, J. E.; Ogliaro, F.; Bearpark, M.; Heyd, J. J.; Brothers, E.; Kudin, K. N.; Staroverov, V. N.; Kobayashi, R.; Normand, J.; Raghavachari, K.; Rendell, A.; Burant, J. C.; Iyengar, S. S.; Tomasi, J.; Cossi, M.; Rega, N.; Millam, J. M.; Klene, M.; Knox, J. E.; Cross, J. B.; Bakken, V.; Adamo, C.; Jaramillo, J.; Gomperts, R.; Stratmann, R. E.; Yazyev, O.; Austin, A. J.; Cammi, R.; Pomelli, C.; Ochterski, J. W.; Martin, R. L.; Morokuma, K.; Zakrzewski, V. G.; Voth, G. A.; Salvador, P.; Dannenberg, J. J.; Dapprich, S.; Daniels, A. D.; Farkas; Foresman, J. B.; Ortiz, J. V.; Cioslowski, J.; Fox, D. J. *Gaussian09*; Gaussian Inc.: Madison, WI, 2010.

(20) (a) Perdew, J. P.; Burke, K.; Ernzerhof, M. *Phys. Rev. Lett.* **1996**, *77*, 3865. (b) Perdew, J. P.; Burke, K.; Ernzerhof, M. *Phys. Rev. Lett.* **1997**, *78*, 1396.

(21) (a) Barone, V.; Cossi, M. *J. Phys. Chem. A* **1998**, *102*, 1995. (b) Cossi, M.; Rega, N.; Scalmani, G.; Barone, V. *J. Comput. Chem.* **2003**, *24*, 669.

(22) Hirata, S.; Head-Gordon, M. *Chem. Phys. Lett.* **1999**, *314*, 291.

(23) (a) Fukui, K. *Acc. Chem. Res.* **1981**, *14*, 363. (b) Hratchian, H. P.; Schlegel, H. B. In *Theory and Applications of Computational Chemistry*; Dykstra, C. E., Frenking, G., Kim, K. S., Scuseria, G. E., Eds.; Elsevier: Amsterdam, The Netherlands, 2005; p 195.

(24) (a) Harvey, J. N.; Aschi, M.; Schwarz, H.; Koch, W. *Theor. Chem. Acc.* **1998**, *99*, 95. (b) Harvey, J. N.; Aschi, M. *Phys. Chem. Chem. Phys.* **1999**, *1*, 5555.

(25) Andrae, D.; Häußermann, U.; Dolg, M.; Stoll, H.; Preuß, H. *Theor. Chim. Acta* **1990**, *77*, 123.

(26) Ehlers, A. W.; Böhme, M.; Dapprich, S.; Gobbi, A.; Höllwarth, A.; Jonas, V.; Köhler, K. F.; Stegmann, R.; Veldkamp, A.; Frenking, G. *Chem. Phys. Lett.* **1993**, *208*, 111.

(27) (a) Hehre, W. J.; Ditchfield, R.; Pople, J. A. *J. Chem. Phys.* **1972**, *56*, 2257. (b) Hariharan, P. C.; Pople, J. A. *Theor. Chim. Acta* **1973**, *28*, 213. (c) Francl, M. M.; Pietro, W. J.; Hehre, W. J.; Binkley, J. S.; Gordon, M. S.; DeFrees, D. J.; Pople, J. A. *J. Chem. Phys.* **1982**, *77*, 3654.

(28) Kasha, M. *Discuss. Faraday Soc.* **1950**, *9*, 14.

(29) Antipas, A.; Dolphin, D.; Gouterman, M.; Johnson, E. C. *J. Am. Chem. Soc.* **1978**, *100*, 7705.

(30) Turro, N. J. *Modern Molecular Photochemistry*; Benjamin/Cummings Publishing: Menlo Park, NJ, 1978.

(31) Khudyakov, I. V.; Serebrennikov, Y. A.; Turro, N. J. *Chem. Rev.* **1993**, *93*, 537.

(32) McMillin, D. R. In *Physical Methods in Bioinorganic Chemistry: Spectroscopy and Magnetism*; Que, L., Jr., Ed.; University Science Books: Mill Valley, CA, 2000; pp 1−58.

DOI: 10.1021/acs.inorgchem.5b00215
Inorg. Chem. 2015, 54, 3624−3630